Biogeosciences Discuss., doi:10.5194/bg-2016-74, 2016
Manuscript under review for journal Biogeosciences
Published: 18 March 2016

Prolonged aragonite undersaturation in bottom water of a biological hotspot in the Chukchi Sea, Arctic Ocean

Michiyo Yamamoto-Kawai [1], Takahisa Mifune [1], Takashi Kikuchi [2], Shigeto Nishiono[2]

[1]Tokyo University of Marine Science and Technology, Tokyo, 108-8477, Japan
[2] Japan Agency for Marine-Earth Science and Technology, Yokosuka, 237-0061, Japan

Correspondence to: Michiyo Yamamoto-Kawai (michiyo@kaiyodai.ac.jp)

Abstract. Distribution of calcium carbonate saturation state (Ω) was observed in bottom waters of the Chukchi Sea in autumn 2012 and early summer 2013. Aragonite and calcite undersaturation were found in high productivity regions in autumn 2012 but not in early summer 2013. Comparison with other parameters has indicated that biological processes -respiration and photosynthesis- are major factor controlling regional and temporal variability of Ω. From these ship-based observations, we have obtained empirical equations to reconstruct Ω from temperature, salinity and apparent oxygen utilization. Using two-year-round mooring data and these equations, we have reconstructed seasonal variation of Ω in bottom water in Hope Valley, a biological hotspot in the southern Chukchi Sea. Results showed prolonged undersaturation for both aragonite and calcite even during winter period, not only in 2012 but also in 2013. Calculations also suggest that bottom water in the hotspot could have been undersaturated for aragonite on an intermittent basis even in the pre-industrial period. Anthropogenic CO_2 has extended the period of aragonite undersaturation to two- or three-fold longer by now. When atmospheric pCO_2 increases to 650 ppm, occupation of aragonite and calcite undersaturation can be as long as two-third and one-third of a year, respectively. Anthropogenic CO_2 has significant impact on duration of $CaCO_3$ undersaturation in the bottom water of the Chukchi Sea, even though horizontal and seasonal variability in Ω is controlled by biological processes.

1 Introduction

During the last decade, ocean acidification due to uptake of anthropogenic carbon dioxide (CO_2) has emerged as an urgent issue in ocean research (e.g., The Royal Society, 2005; Orr et al., 2005). Increasing acidity and consequent changes in seawater chemistry are expected to impact marine ecosystem and may threaten some organisms (e.g., Gattuso and Hansson 2011; Branch et al. 2013). Of particular concern is the impact of ocean acidification on calcifying organisms, such as coralline algae, pteropods, bivalves, corals etc., because acidification lowers the saturation state (Ω) of calcium carbonate ($CaCO_3$) in seawater to affect the ability of these organisms to produce and maintain their shells or skeletons (e.g., Kroeker et al. 2013 and references therein). In fact, a decrease in Ω of bottom water can cause enhanced mortality of juvenile shellfish (Green et al., 2009; Talmage and Gobler, 2009) and decreased calcification, growth, development and abundance of calcifiers (Kroeker et al., 2013).

The shallow shelf seas of the Arctic Ocean are known to be especially vulnerable to ocean acidification. Cold water dissolves more CO_2, large freshwater inputs from rivers and sea ice melt reduce calcium ion concentrations and alkalinity, the buffering capacity of seawater to added CO_2 (Sulisbury, 2008; Yamamoto-Kawai et al., 2011), and respiration at the bottom of salt stratified water column accumulates CO_2 in bottom water (Bates et al., 2009). Because of these characteristics, both surface and bottom waters of Arctic shelf seas exhibits naturally low Ω compared to other ocean waters (e.g., Fabry et al., 2009; Mathis et al., 2015; Yamamoto-Kawai et al., 2013). The Chukchi Sea is one of these seas.

The Chukchi Sea is a vast and shallow shelf sea north of the Bering Strait. Nutrients upwelled onto the Bering shelf is carried by northward flowing Pacific-origin water to the Chukchi Sea, making the sea to have very high primary productivity (e.g., Springer and McRoy, 1993). Large proportion of produced organic matter is directly delivered to the seabed, due to shallow bottom depth and mismatch between seasonal dynamics of phytoplankton and zooplankton (e.g., Grebmeier et al., 2006). Exported organic matter is remineralized back to CO_2 at depth and lowers Ω of bottom water (e.g., Bates et al., 2009). At the same time, high export rate of organic matter supports very high benthic biomass that are prey for higher trophic levels such as diving ducks, seals, whales and walruses (Grebmeier et al., 2006; Fabry et al., 2009). Because calcifying bivalves, amphipods, brittle stars and crabs are dominant spices in benthic community of the Chukchi Sea (Fabry et al.,2009; Blanchard et al., 2013), they are key component of the ecosystem. Ocean acidification, therefore, could have considerable impacts on the ecosystem and biogeochemical cycles of the Chukchi Sea. In addition, because of shallow bottom depth of ~50 m, anthropogenic CO_2 can immediately penetrate into bottom water to which benthos are exposed.

Recent studies have found bottom waters already undersaturated with respect to aragonite-type $CaCO_3$ in the Chukchi Sea during summer and autumn (Bates et al., 2009; 2013; Bates, 2015; Mathis et al., 2014). Bates et al. (2013) reported that ~40% of sampled bottom waters during summertime cruises between 2009 and 2011 were aragonite-undersaturated. Some bottom waters were also undersaturated with respect to calcite, a less soluble form of $CaCO_3$ than aragonite. These studies indicate that benthic communities in large areas of this shelf sea has been exposed to bottom waters that are corrosive for their CaCO3 shells and skeletons, at least seasonally. However, full seasonal variation of Ω is still unrevealed due to difficulties in shipboard observations during ice-covered months. Because many organisms may be more vulnerable during early development stages and many benthic organisms have planktonic larval stages (e.g., Talmange and Gobler, 2009), timing and duration of $CaCO_3$ can be critical for their growth and populations.

In the present paper, we show distribution of Ω in bottom water of the Chukchi Sea in September of 2012 and July of 2013 and discuss factors controlling Ω. Based on these observations, we reconstruct seasonal variations of Ω in the bottom water by using data from a mooring observation between July 2012 and July 2014 in Hope Valley, a biological "hotspot" in the southern Chukchi Sea (Grebmeier et al., 2006; Nishino et al., 2016).

2 Observation and analysis

Hydrographic data were collected in the Chukchi and Bering Seas during the cruises of R/V Mirai of the Japan Agency for Marin-Earth Science and Technology (JAMSTEC) from 13 September to 4 October in 2012 (Kikuchi et al., 2012) and T/S

Oshoro-Maru of Hokkaido University from 3 July to 18 July in 2013 (Hirawake et al., 2013). In the present paper, we use data from stations north of 66°N with bottom depth shallower than 70 m. During both cruises, hydrographic casts was performed using a Sea Bird 9plus CTD to which a carousel water sampler with Niskin bottles was mounted. Seawater samples were collected for total alkalinity (TA) and dissolved inorganic carbon (DIC) as well as complementary data (S: salinity, T: temperature, DO: dissolved oxygen, and nutrients). Samples for TA and DIC were collected according to Dickson et al. (2007). TA was measured using a spectrophotometric system (Yao and Byrne, 1998) for samples from Mirai and an open cell titration system (Dickson et al., 2007) for samples from Oshoro-Maru. DIC from both cruises were analyzed using a coulometer system. Measurements of TA and DIC were calibrated against a certified reference material distributed by A. G. Dickson at Scripps Institute of Oceanography, or General Environmental Technos Co.. The pooled standard deviation (Sp) for duplicate samples was < 2.2 μmol kg^{-1} and < 5.5 μmol kg^{-1} for TA and DIC, respectively. Observations of TA, DIC, nutrients, T, S and pressure were used to calculate Ω for aragonite (Ωar) or calcite (Ωca) and pCO_2 (partial pressure of CO_2) by using the CO2sys program (Lewis and Wallace, 1998) with constants of Lueker et al. (2000) for K1 and K2 and Dickson (1990) for KSO_4.

A mooring system was deployed in Hope Valley from 16 July 2012 to 19 July 2014. The system was first deployed at 67º 42’N, 168º 50’W from 16 July 2012 to 2 October 2012, and then moved slightly to the north at 68º 02’N, 168º 50’W on 3 October 2012. On 20 July 2013, the system was recovered for the maintenance and redeployed at the latter location until 19 July 2014. Bottom depth was 52, 59 and 60 m, respectively for each deployment. Sensors for T, S, DO, chlorophyll a and turbidity were equipped on the mooring at 7 m above from the bottom. Data were recorded every hour. Details of sensor and mooring observations are described in Nishino et al. (2016).

3 Results and discussions

3.1 Ship-based observations

Distributions of Ω in bottom waters of the Chukchi Sea (Fig. 1) were significantly different between September/October 2012 (hereafter autumn 2012) and July 2013 (hereafter summer 2013). In autumn 2012, Ω in bottom water ranged from 0.3 to 2.0 for aragonite and from 0.5 to 3.2 for calcite. Aragonite undersaturation (Ωar < 1; black circles in Fig. 1) was observed at stations off Pt. Barrow, in Hope Valley, in Bering Strait, and near the northern continental slope. The lowest Ωar was observed on 3 October 2012 in Hope Valley at 68ºN, in the dome-like structure of bottom water with low T, high S and low DO (Fig. 2; Nishino et al., 2016). Calcite undersaturation was also found in this dome in Hope Valley (Figs. 1b and 2). Nishino et al. (2016) describe that the dome-like structure is a common feature found in this region associated with Hope Valley topographic depression, although water properties can differ between years and seasons. Note that stations along 168 °W in Hope Valley were visited twice on 13-17 September and 3-4 October in 2012 and difference in Ω values of bottom water between two visits (< 0.2) were smaller than differences between stations inside and outside of the dome-like structure (~0.7).

In summer 2013, all of observed waters were oversaturated with respect to aragonite and calcite (Figs. 1c and 1c). Although stations in Hope Valley again showed the dome-like feature with low T and low DO, they were not as prominent as in 2012

(Fig. 2). Ω in bottom waters at these stations were slightly lower than stations north or south but still well oversaturated with respect to $CaCO_3$ (Ωar =1.7 ~1.9; Ωca =2.8 ~3.0). Waters with lower Ωar of 1.1~1.2 and Ωca of 1.8 ~1.9 were found in northern stations at around 71°N where T and DO were also lower than in the south.

In both years, low Ω was observed in bottom waters with low T, low DO and high S. Figure 3 shows relationships between Ωar and T, S or apparent oxygen utilization (AOU; difference between saturation and observed concentrations of DO). Ωar showed the highest correlation with AOU and data from two cruises were distributed on a line in the Ωar-AOU diagram (Fig. 3). AOU is a measure of how much oxygen has been consumed by respiration and decomposition of organic matter in the water column. Accordingly, high AOU corresponds to high pCO_2 and therefore low Ω. Negative AOU value is a sign of photosynthesis which produces DO and consumes CO_2 to increases Ω.

Ωar increased with increasing T and regression lines for two cruises were similar in slope but different in intercept (Fig. 3). Ωar also increased with decreasing S in bottom waters, whereas Ωar decreased with decreasing S in upper waters (Fig. 3). The latter is explained by mixing with freshwater, which lowers calcium ion concentration and alkalinity to decrease Ωar as indicated by previous studies (Salisbury et al., 2008; Yamamoto-Kawai et al., 2009). In fact, aragonite undersaturation were observed in very low S surface waters in 2012 (Fig. 3). The opposite relationship in bottom waters is probably because higher bottom S creates stronger stratification of water column that prevent release of CO_2 produced by respiration at depth. These results show that variations in Ω in the Chukchi Sea bottom water is controlled largely by organic matter remineralization with minor contributions of T and S. This is consistent with previous studies that have pointed out the importance of high primary production and remineralization of exported organic matter to induce undersaturation of $CaCO_3$ in bottom waters of the Chukchi Sea (Bates et al., 2009; 2013; Bates, 2015). In fact, low Ω waters were observed in regions off Pt. Barrow and Hope Valley, known as biological "hotspots" in the Chukchi Sea, characterized by high primary productivity, high export flux of organic matter to depth, high respiration rate in sediment community, and high benthic biomass (Grebmeier et al., 2006; Nishino et al., 2016).

In autumn 2012, Ω was much lower than in summer 2013, not only in bottom water but for the whole water column (Fig. 2). Nishino et al. (2016) compared hydrographic conditions in this area in late summer of 2004, 2008, 2010, 2012 and 2013, and found that 2012 was unusual year with strong stratification, due to an input of sea ice meltwater, and with remarkably low DO concentration at depth. Stronger stratification should prevent ventilation and accumulate more CO_2 in the bottom water. This explains high AOU and low Ω in bottom water in autumn 2012 (Fig. 2). Seasonal variation in Ω should also be a cause of the difference between two observations as described in the following sections. In upper layers of the water column, lower Ω in 2012 relative to S and T than in 2013 (Fig. 3) might be due to low photosynthetic activity associated with stronger stratification and to mixing with sea ice meltwater (Nishion et al., 2016). In addition, input of sea ice meltwater itself lowered Ω in surface waters in 2012 as evident in Fig. 3b. The fact that ranges of T and S for bottom waters were not significantly different between two cruises (Fig. 3) indicates that the accumulation of more CO_2 produced by respiration was the major cause of the much lower Ωar in autumn 2012 than summer 2013.

3.2 Mooring observations

Mooring data revealed seasonal variation in T, S, DO and AOU in bottom water in Hope Valley where aragonite and calcite undersaturations were observed in autumn 2012 (Fig. 4). Ship-based observations were made near the mooring site (~68ºN) on 14 September 2012, 3 October 2012 and 16 July 2013 and agreed well with sensor data. T, S and DO (AOU) ranged from -1.92 to 2. 73, 30.41 to 35.49, and 62.66 to 416.39 (-32.66 to 294.92), respectively. Note that ship-based observations captured both higher and lower ends of seasonal variation in DO. During summer/autumn months, T, S and DO showed large and high frequent variability. Because all three parameters changed simultaneously, this is likely due to changes in water current which carries water masses with different characteristics from surrounding areas. This also indicates horizontal inhomogeneity of bottom water properties during summer/autumn.

T was high in summer/autumn months, decreased from October to December due to atmospheric cooling, and kept at near freezing temperature (~ -1.8 °C) from January to May. Summer/autumn T was lower in 2012 than in 2013. Stronger stratification of water column due to a meltwater input in 2012 (Nishino et al., 2016) may be the cause of this difference. This is also consistent with higher S in bottom water in 2012 than in 2013. Mean S for the whole observation period was 32.4. In both years, freshening was observed at the beginning of the cooling period, because of mixing of low-S upper waters into the bottom layer by vertical convection (Woodgate et al., 2005). Another freshening was also found at the beginning of warming periods due to melting of sea ice (Woodgate et al., 2005). In winter of 2013, S increased rapidly in February to as high as 35.49 and then decreased sharply in March. This suggests an advection of water mass from active ice formation area, such as coastal polynya region where brine rejection from freezing seawater increases S of bottom water to form "hypersaline water" (Weingartner et al., 1998). Such event was not observed in the following winter.

DO increased and reached supersaturation (negative AOU) in May and June (Fig. 4), accompanied by a sharp increase in chlorophyll-a concentration (Nishino et al., 2016), indicating effects of oxygen production by photosynthesis even in the bottom water. DO then decreased from ~300 μmol kg^{-1} in July to ~125 μmol kg^{-1} in September 2012 and to ~225 μmol kg^{-1} in September 2013 (Fig. 4). DO was kept low until the onset of winter convection in October/November. As mentioned in the previous section, DO in bottom water was unusually low in autumn 2012, due to strong stratification that prevented ventilation of bottom water. During winter, DO was relatively stable at ~325 μmol kg^{-1}. This concentration corresponds to ~50 μmol kg^{-1} in AOU and ~85 % in saturation level, indicating undersaturation of DO during winter even in the hypersaline water that is formed in contact with atmosphere. This suggests that DO undersaturation in winter bottom water is not due to insufficient gas exchange, but to continued consumption of oxygen by benthic organisms during winter. In fact, Devol et al. (1997) reported that benthic oxygen consumption rate in winter was half of or comparable to that in summer in coastal area north of Pt. Barrow, Alaska.

The analysis of mooring data indicates that our ship-based observations in summer 2013 captured bottom water that was under the influence of photosynthesis. In autumn 2012, on the other hand, we have observed bottom water that was largely affected by organic matter decomposition. This explains the differences in AOU and Ωar in bottom water between two ship-based observations in September/October 2012 and July 2013.

3.3 Regression analysis

Based on ship-based and mooring observations, we reconstruct seasonal evolution of Ω in the bottom water of Hope Valley. Previous studies have used multiple linear regression models to robustly determine carbonate parameters such as DIC, TA, Ω, and pH from observations of T, S, DO or nutrients (Juranek et al., 2009; Alin et al., 2012). These empirical equations were successfully used to reconstruct seasonal and interannual cycles, as well as high-frequency variability in short-time scales (Juranek et al., 2009; Alin et al., 2012; Leinweber and Gruber, 2013; Evans et al., 2013). In the present study, we employ a similar approach to estimate Ω. We use observations from two cruses to determine regression equations for DIC and TA using T, S and AOU as input parameters. The goodness of the fit was assessed by correlation coefficients (r^2) and root mean square error (RMSE). AOU, not DO itself, is used as a measure of biological process because DO concentration changes with T and S. We then calculate Ω from estimated TA and DIC with observed T, S and pressure, rather than directly estimate Ω from input parameters. In this way, we can take into account the effects of T, S and pressure on solubility of $CaCO_3$ (Mucci 1983; Millero 1995).

DIC is controlled by physical (solubility and gas exchange) and biological processes (photosynthesis and respiration) and therefore is a function of T, S and AOU. TA in the study area is a function of S, as it is determined by mixing of Pacific-origin seawater with freshwater and formation of sea ice (brine rejection increase both S and TA of the underlying water). Mixing between sea water and freshwater sources with different TA (high in river and low in sea ice meltwater and precipitation; Yamamoto-Kawai et al., 2005) is evident in the S-TA diagram (not shown) but only in surface waters with S < 31.

The best predictions for DIC and TA (DICest and TAest) were obtained when all three parameters were used: DICest = 1.06 × AOU - 17.03 × T + 41.54 × S + 743.94 (r^2=0.96, RMSE=24.46, n=184) and TAest = 0.04 × AOU – 4.24 × T + 45.34 × S + 760.35 (r^2=0.85, RMSE=13.13, n=184). However, because warming or cooling do not directly alter TA, observed correlation between TA and T should reflect characteristics of different water masses. Thus this relationship may not hold for other seasons in this shallow shelf sea where cooling or warming can significantly change T in the bottom water without changing TA. For estimation of TA, therefore, we decided to use a regression equation only with S: TAest = 59.23 × S + 370.34 (r2=0.83, RMSE=14.03, n=184). Although biological activities can change TA in small extent by adding or removing nitrate or ammonium, the inclusion of AOU did not significantly improve the regression model (r^2=0.83, RMSE=14.06).

Figure 5a shows a good linear correlation between observations (Ωobs) and estimations (Ωest) with r2 =0.94 for aragonite (r2 =0.94 calcite, not shown). Larger differences between two values were found in surface waters with Ωest values higher than 2.5 for aragonite and 4.0 for calcite. Including these samples, RMSE was 0.17 for Ωar and 0.28 for Ωca (n = 184). In order to evaluate obtained regression equations, we have applied the same equations to independent data from R/V Mirai cruises in the Chukchi Sea in 2000, 2002, 2006, 2009 and 2010, downloaded from the website of Japan Agency for Marine-Earth science and Technology (JAMSTEC). These cruise observations were carried out in August, September or October. Total 127 samples with S > 31 and with observations of DIC and TA were found in the study area (latitude> 66°N, bottom depth < 70 m). Ω calculated from DICest and TAest (Ωest) was well correlated with observed Ω (Ωobs) with a regression equation of Ωarest = 1.15 ×Ωarobs - 0.04 (r^2 = 0.77, RMSE=0.36, Fig. 5b) and Ωcaest = 1.14 ×Ωcaobs - 0.06 (r^2 = 0.77, RMSE=0.57). These RMSE values were regarded as errors in reconstructed Ω in the following section.

Cross et al. (2013) pointed out the possibility of shallow-water $CaCO_3$ mineral dissolution, which could cause an increase in TA by 36 umol kg^{-1} in the northern Bering Sea where aragonite undersaturation lasts for 5 months from spring to autumn. In our study area, an increase in TA was also found in some bottom waters. However, this was likely due to brine injection, rather than mineral dissolution. This was suggested by a comparison of S, TA and oxygen isotope ratio of water ($\delta^{18}O$) observed in cruises of R/V Mirai in 2000, 2002, 2009, 2010 and 2012 in the Chukchi Sea. The increase in TA was correlated with brine content, estimated from $\delta^{18}O$ as shown in Yamamoto-Kawai et al. (2005), rather than with Ω of the water. Therefore, we consider that effect of mineral dissolution is insignificant in waters discussed in our analysis.

3.4 Seasonal variation of Ω in Hope Valley bottom water

Based on the analysis in the section 3.3., the regression equations for DIC and TA were applied to the mooring data in Hope Valley, a biological hotspot in the Chukchi Sea. Waters with S < 31 were intermittently observed between 8 and 21 November 2013 and excluded from the analysis. Reconstructed variation of is shown in Fig. 6 with ±0.36 for aragonite and ±0.57 for calcite. For the whole period, Ωest ranged from 0.2 to 2.1 for aragonite and from 0.3 to 3.4 for calcite (Fig. 6). It was shown that our ship-based observations in autumn 2012 and summer 2013 have captured the lowest and the highest Ω periods, respectively. Seasonal variation of Ω mirrors that of DO, low in autumn due to stratification and respiration and high in spring due to photosynthesis. In autumn 2012, the unusually stratified year, bottom water Ω was ~0.3 for aragonite and ~0.5 for calcite. The lowest value of 0.2 and 0.3, respectively, was found on 27 November. In autumn 2013, Ω was higher than in 2012 but was still below 1 for aragonite for most of the days in August, September and October. At the beginning of cooling and convection period in November/December 2012 and October/November 2013, ventilation of bottom water increased DO and Ω. Then, bottom water was kept at aragonite undersaturation for most of the winter until the start of photosynthesis in May. Even during spring and early summer months, intermittent undersaturation was found, showing inhomogeneous distribution of undersaturated waters during this period. In winter, in contrast, variability in Ω is relatively small. This suggest that undersaturation occurs not only at the mooring site in a hotspot but also in surrounding areas during winter. Relatively low Ω in winter is likely due to continued respiration and organic matter decomposition by benthic organisms during winter (Devol et al., 1996) as suggested by positive AOU. An exception is the hypersaline water that could have high calcium ion concentrations and alkalinity concentration to result in high Ω. However, S of this water is out of the range of ship-based observations used for multiple linear regression analysis, and thus Ω of this water is not very reliable.

Reconstructed Ω showed a prolonged and frequent aragonite undersaturation in the bottom water of the Chukchi Sea, not only in summer/autumn but also in winter months. In previous studies, continuous aragonite undersaturation has been observed in bottom waters in Bering and Chukchi Sea but limited in seasons. Cross et al. (2013) reported persisted aragonite undersaturation of bottom water of the northern Bering Sea shelf for at least 5 months from mid-April to early October in 2009. Mathis et al. (2014) indicated sustained bottom aragonite undersaturation on the southern Bering Sea shelf for at least of 4 months from mid-June to early October in 2011. In the Northern Chukchi Sea around 71.5°N and 165°W, Mathis and Questel (2013) observed seasonal changes in Ωar and reported that bottom water became partially undersaturated in September and broadly undersaturated in October in 2010, with a lowest Ωar value of ~0.7. The present study is the first to estimate year-round variability of Ω in the bottom water of the Chukchi Sea. For the first (from 16 July 2012 to 16 July 2013) and second (from 16 July 2013 to 16 July 2014) full-year mooring observations, total hours of aragonite undersaturation was counted to be 6258 hours and 5320 hours, respectively. These corresponds to 261 days, 8.5 months or 71 % of a year for the first year, and 221 days, 7.3 months or 61 % of a year for the second year. For calcite, undersaturation was not as frequent as aragonite (Fig. 6) but found not only for the unusual autumn 2012 but also in 2013 on an intermittent basis. Total hours of calcite undersaturation was 2252 hours (94 days, 3 months, 26 % of a year) and 545 hours (23 days, 0.7 month and 6 % of a year) for first and second year, respectively. Considering that the mooring site is located in a biological hotspot where the lowest Ω was observed in autumn (Figs. 1 and 2), total hours of undersaturation estimated here is likely at a maximum within the Chukchi Sea.

3.5 Anthropogenic impact on Ω

In order to quantify the effect of anthropogenic CO_2 on our 2-year time series of Ω, we have followed previous studies (Gruber et al., 1996; Sabine et al., 1999; Yamamoto-Kawai et al., 2013; 2015). DIC concentration observed in year t-obs can be expressed as:

$$DICt\text{-}obs = DICEQt\text{-}0 + (\Delta diseq + \Delta bio)$$

Where DICEQt-0 is DIC of seawater in equilibrium with the atmospheric CO_2 in the year t-0 when the water parcel was last in contact with the atmosphere, Δdiseq and Δbio represents air-sea equilibrium at the surface and change in DIC due to biological activity. In case of the shallow Chukchi Sea shelf, t-0 can be assumed to be the observed year t-obs and therefore the sum of the last two terms can be calculated by comparing observed DIC and DICEQ for the year t-obs. In calculating DICEQt-0, we have used pCO_2 of 380 ppm. Then, assuming that Δdiseq and Δbio do not change with time, DIC in any year t can be estimated by using atmospheric pCO_2 at the year t. We have estimated Ω with DICt for the pre-industrial period when pCO_2 was 280 ppm, and for the year 2066, 50 years after the present when pCO_2 reaches 650 ppm in the high CO_2 emission scenario (RCP8.5, Riahi et al., 2011).

Figure 7 shows time-series of Ω for the case of pre-industrial period and that of 50 years later at the mooring site. For the former case, Ω ranged from 0.2 to 2.6 for aragonite and from 0.4 to 4.1 for calcite. For the latter case, Ω ranged from 0.2 to 1.5 for aragonite and from 0.2 to 2.4 for calcite. Caveat here is that our calculation is based on an assumption that terms Δdiseq and Δbio have not changed since pre-industrial period. As biological process is the major factor changing DIC in bottom water, changes in Δbio can cause significant error in estimated Ω for the past and the future. For example, if biological production and subsequent remineralization at depth is lower in the past or in the future, Ω should be higher than shown in Fig. 7. At the moment, unfortunately, trends in productivity in the southern Chukchi Sea is still under debate. Lee et al. (2007) and Yun et al., (2014) show that primary production rate in recent years are lower than previous estimates made in 1990s. From chlorophyll a analysis, Grebmeier et al. (2012) and Arrigo and van Dijken (2011) have suggested an increase in primary productivity in 2000s in the Chukchi Sea. Grebmeier et al. (2015) also showed an increase in benthic biomass from 1970s to 2010 followed by a decline between 2010 and 2012 in our study area. To get a rough idea, we have calculated Ω for pre-industrial case with (Δdiseq + Δbio) term half of that at present. Because Δdiseq should be much smaller than Δbio in our highly productive study area, this is considered to represent half productivity and half respiration than today. With half biological activity, Ω is estimated to range from 0.6 to 2.2 for aragonite and from 1.0 to 3.5 for calcite in pre-industrial case. This means that $CaCO_3$ undersaturation of bottom water of biological hotspot might have occurred, at least for aragonite, even with half productivity than today and without perturbation by anthropogenic CO_2. This may be the case only in hotspots or only in our study site, because previous studies in the Chukchi Sea have suggested that undersaturation in bottom water is a recent phenomenon caused by anthropogenic CO_2 (Bates et al., 2009; 2013; Mathis and Questel, 2013).

In terms of duration, aragonite (calcite) undersaturation occupies 33 % (22 %) and 16 % (3 %) of the first and second year, respectively, in the case of pre-industrial period with no change in productivity. By comparing with original estimate for 2012 and 2013, it is indicated that anthropogenic CO_2 has largely increased the period of aragonite undersaturation in the study site from 33 % to 71% and from 16 % to 61 %. In the future case with atmospheric pCO_2 of 650 ppm, occupation of aragonite undersaturation increases to 99 % and 66 % for the first and second year, respectively. Calcite undersaturation occupies 75 % and 38 % of the first and second year, respectively. These analysis indicate that anthropogenic CO_2 has significant impact on saturation condition of $CaCO_3$ in the bottom water even though seasonal and interannual variations of Ω is mainly controlled by biological processes.

4 Summary and conclusions

Horizontal distribution of Ω in bottom water of the Chukchi Sea was observed in autumn 2012 and early summer 2013. Both aragonite and calcite undersaturation was observed in highly productive regions, including Hope Valley, but only in 2012. Comparison with AOU, T and S showed that organic matter remineralization is the major factor controlling Ω of bottom water in the Chukchi Sea, with minor but significant control of T and S.

We also performed mooring observation of AOU, T and S for two years in Hope Valley, a biological hotspot, where lowest Ω was observed in cruise observations in 2012. Mooring data revealed that our ship-based observations captured conditions at both ends of seasonal and interannual variations in biological processes: under very strong influence of remineralization in autumn 2012, and under the photosynthesis in early summer 2013. This explains large difference in Ω between two cruises.

Using cruise observations, we have obtained empirical equations to reconstruct Ω from data of T, S and AOU and applied them to mooring data in Hope Valley. Reconstructed variation of Ω in bottom water of this biological hotspot showed prolonged undersaturation for both aragonite and calcite, not only in 2012 but also in 2013. Aragonite undersaturation occupied more than 60 % of a year. Occupation of calcite undersaturation was 26 % for highly stratified first year and 6 % in second

year. Such prolonged aragonite undersaturation may be harmful for benthic calcifiers who rely on a planktonic early life stages with shells composed of aragonite. Calculations suggest that bottom water in the hotspot could have been aragonite undersaturation on an intermittent basis even in the pre-industrial period. It was also suggested that anthropogenic CO_2 has extended the period aragonite undersaturation to two- or three-fold longer by now. Calcite undersaturation period was also extended to about two-hold longer than pre-industrial period. With increased atmospheric pCO_2 of 650 ppm, occupation of aragonite undersaturation should increase to more than two-third of a year, with possibility of almost year-long occupation under highly stratified condition. Occupation of calcite undersaturation will also increase to more than one-third of a year. Surely, anthropogenic CO_2 has significant impact on duration of $CaCO_3$ undersaturation in the bottom water even though seasonal and interannual variations in Ω is controlled by biological processes.
It has been revealed that $CaCO_3$ undersaturation has negative impacts on calcifying organisms (e.g., Kroeder et al., 2013). Therefore, continuous occurrence of undersaturation since pre-industrial period in a biological hotspot in the southern Chukchi Sea may be conflicting the fact that bivalves are dominant in benthic community in this area (Grebmeier et al., 2012; 2015). In fact, when we collected benthic organisms by using a dredge during the cruise of T/S Oshoro-maru in 2013, many bivalves were found in Hope Valley hot-spot area, both well-grown adults and small young individuals (Fig. 8). This may suggest tolerance of these bivalves to $CaCO_3$ undersaturation with protection mechanisms such as external organic layer (Ries et al., 2009), companion of energetic cost of calcification by abundant supply of food (Wood et al., 2008), migration, or mismatch in timing of their planktonic and settling stages and occurrence of $CaCO_3$ undersaturation in surrounding water. With rapidly increasing anthropogenic CO_2 in recent and future years, quantification of the responses of local calcifying organisms to low Ω is an urgent issue for the future study. A biological hotspot of the Chukchi Sea, with already prolonged $CaCO_3$ undersaturation, should provide a research field to assess vulnerability and resilience of organisms to ocean acidification, or to find direct evidence of consequences of ocean acidification in Arctic seas.

References

This work was done as a part of the "Arctic Climate Change Research Project" within the framework of the Green Network of Excellence (GRENE) Program funded by the Ministry of Education, Culture, Sports, Science and Technology-Japan (MEXT). We thank captains, officers and crews of R/V Mirai, Japan Agency for Marine-Earth Science and Technology (JAMSTEC), T/S Oshoro-Maru, Hokkaido University, and CCGS S. W. Laurier for their help in sampling and mooring operations. Data from these cruises are, or will be, available at website of JAMSTEC and/or Arctic Data archive System (ADS), Japan. Also used in this study are data acquired during the MR00-K06, MR02-K05, MR06-04, MR09-03, MR10-05 and MR12-E03 cruise of R/V Mirai, downloaded from the JAMSTEC website. Oxygen isotope ratio of waters collected during R/V Mirai 2012 cruise was provided by Dr. Zhan at Toyama University. Some figures in this paper were illustrated using Ocean Data View software (R. Schlitzer, 2008, available at http://odv/awi.de/).

References

Alin, S. R., Feely, R. A., Dickson, A. G., Hernández‐Ayón, J. M., Juranek, L. W., Ohman, M. D., and Goericke, R.: Robust empirical relationships for estimating the carbonate system in the southern California Current System and application to CalCOFI hydrographic cruise data (2005–2011), J. Geophys. Res., 117, C05033, doi:10.1029/2011JC007511, 2012.

Arrigo, K. R., and van Dijken, G. L.: Secular trends in Arctic Ocean net primary production, J. Geophys. Res., 116, C09011, doi:10.1029/2011JC007151, 2011.

Bates, N. R., Orchowska, M. I., Garley, R., and Mathis, J. T.: Summertime calcium carbonate undersaturation in shelf waters of the western Arctic Ocean-how biological processes exacerbate the impact of ocean acidification, Biogeosci., 10, 5281-5309, 2013.

Bates, N. R., Mathis, J. T., and Cooper, L. W.: Ocean acidification and biologically induced seasonality of carbonate mineral saturation states in the western Arctic Ocean, J. Geophy. Res., 114, C11007, doi:10.1029/2008JC004862, 2009.

Bates, N. R.: Assessing ocean acidification variability in the Pacific-Arctic region as part of the Russian-American Long-term Census of the Arctic, Oceanogr., 28, 36-45, 2015.

Blanchard, A. L., Parris, C. L., Knowlton, A. L., and Wade, N. R.: Benthic ecology of the northeastern Chukchi Sea. Part I. Environmental characteristics and macrofaunal community structure, 2008–2010, Continental Shelf Res., 67, 52-66, 2013.

Branch, T. A., DeJoseph, B. M., Ray, L. J., and Wagner, C. A.: Impacts of ocean acidification on marine seafood, Trends Ecol. Evol., 28, 178-186, 2013.

Cross, J. N., Mathis, J. T., Bates, N. R., and Byrne, R. H.: Conservative and non-conservative variations of total alkalinity on the southeastern Bering Sea shelf, Mar. Chem., 154, 100-112, 2013.

Devol, A. H., Codispoti, L. A., and Christensen, J. P.: Summer and winter denitrification rates in western Arctic shelf sediments, Continental Shelf Res., 17, 1029-1050, 1997.

Dickson, A. G., Sabine, C. L., and Christian, J. R.: Guide to best practices for ocean CO_2 measurements, PICES Special Publications, 3, 191pp, 2007.

Dickson, A. G.: Standard potential of the reaction: AgCl (s)+ 1/2H2(g)= Ag(s)+ HCl(aq), and the standard acidity constant of the ion HSO_4^- in synthetic sea water from 273.15 to 318.15 K, J. Chem. Thermodynamics, 22, 113-127, 1990.

Evans, W., Mathis, J. T., Winsor, P., Statscewich, H., and Whitledge, T. E.: A regression modeling approach for studying carbonate system variability in the Northern Gulf of Alaska, J. Geophys. Res., 118, 476-489, 2013.

Fabry, V. J., McClintock, J. B., Mathis, J. T., & Grebmeier, J. M.: Ocean acidification at high latitudes: the bellwether, Oceanogr., 22, 160-171, 2009.

Gattuso, J. P., Hansson, L.: Ocean acidification, Oxford University Press, 311pp., 2011.

Grebmeier, J. M.: Shifting patterns of life in the Pacific Arctic and Sub-Arctic seas, Mar. Sci., 4, 63-78, 2012.

Grebmeier, J. M., Bluhm, B. A., Cooper, L. W., Denisenko, S. G., Iken, K., Kędra, M., and Serratos, C.: Time-series benthic community composition and biomass and associated environmental characteristics in the Chukchi Sea during the RUSALCA 2004–2012 Program, Oceanogr., 28, 116-133, 2015.

Grebmeier, J. M., L. W. Cooper, H. M. Feder, and B. I. Sirenko: Ecosystem dynamics of the Pacific-influenced Northern Bering and Chukchi Seas in the Amerasian Arctic, Prog. Oceanogr., 71, 331-361, 2006.

Green, M. A., Waldbusser, G. G., Reilly, S. L., Emerson, K., and O'Donnell, S.: Death by dissolution: sediment saturation state as a mortality factor for juvenile bivalves, Limnol. Oceanogr., 54, 1037-1047, 2009.

Gruber, N., Sarmiento, J. L., and Stocker T. F.: An improved method for detecting anthropogenic CO_2 in the oceans, Global Biogeochem. Cycles, 10, 809-837, 1996.

Hirawake, T.: Cruise Report, Training Ship Oshoro Maru Cruise No. 255, Hokkaido University, Japan, 2013.

Juranek, L. W., Feely, R. A., Peterson, W. T., Alin, S. R., Hales, B., Lee, K., Sabine, C. L., and Peterson, J.: A novel method for determination of aragonite saturation state on the continental shelf of central Oregon using multi−parameter relationships with hydrographic data, Geophys. Res. Lett., 36, L24601, doi:10.1029/2009GL040778, 2009.

Kikuchi, T. :R/V Mirai Cruise Report MR12-E03, JAMSTEC, Yokosuka, Japan. http://www.godac.jamstec.go.jp/darwin/e, 2012.

Kroeker, K. J., Kordas, R., Crim, R., Hendriks, I. E., Ramajo, L., Singh, G. S., Duarte, C. M. Gattuso, J. P.: Impacts of ocean acidification on marine organisms: quantifying sensitivities and interaction with warming, Global Change Boil., 19, 1884-1896, 2013.

Lee, S. H., Whitledge, T. E., and Kang, S. H.: Recent carbon and nitrogen uptake rates of phytoplankton in Bering Strait and the Chukchi Sea, Continental Shelf Res., 27, 2231-2249, 2007.

Leinweber, A., and Gruber, N.: Variability and trends of ocean acidification in the Southern California Current System: A time series from Santa Monica Bay, J. Geophys. Res., 118, 3622-3633, 2013.

Lewis, E., and Wallace, D. W. R.: Program Developed for CO_2 System Calculations, ORNL/CDIAC-105, Carbon Dioxide Information Analysis Center, Oak Ridge National Laboratory, U.S. Department of Energy, Oak Ridge, Tennessee. doi: 10.3334/CDIAC/otg.CO2SYS_DOS_CDIAC105, 1998.

Lueker, T. J., Dickson, A. G. and Keeling, C. D.: Ocean pCO_2 calculated from dissolved inorganic carbon, alkalinity, and equations for K_1 and K_2: validation based on laboratory measurements of CO_2 in gas and seawater at equilibrium, Mar. Chem. 70, 105–119, 2000.

Day, R. H., Weingartner, T. J., Hopcroft, R. R., Aerts, L. A., Blanchard, A. L., Gall, A. E., Gallaway, B. J., Hannay, D. E., Holladay, B. A., Mathis, J. T., Norcross, B. L., Questel, J. M., and Wisdom, S. S.: The offshore northeastern Chukchi Sea, Alaska: a complex high-latitude ecosystem, Continental Shelf Res., 67, 147-165, 2013.

Mathis, J. T., Cross, J. N., Evans, W., and Doney, S. C.: Ocean acidification in the surface waters of the Pacific-Arctic boundary regions, Oceanogr., 28, 36-45, 2015.

Mathis, J. T., Cross, J. N., Monacci, N., Feely, R. A., and Stabeno, P.: Evidence of prolonged aragonite undersaturations in the bottom waters of the southern Bering Sea shelf from autonomous sensors, Deep Sea Res., 109, 125-133, 2014.

Mathis, J. T., and Questel, J. M.: Assessing seasonal changes in carbonate parameters across small spatial gradients in the Northeastern Chukchi Sea. Continental Shelf Res., 67, 42-51, 2013.

Millero, F. J.: Thermodynamics of the carbon dioxide system in the oceans, Geochimica osmochimica Acta, 59, 661-677, 1995.

Mucci, A.: The solubility of calcite and aragonite in seawater at various salinities, temperatures and atmosphere total pressure, Am. J. Sci., 238, 780–799, 1983.

Nishino, S., Kikuchi, T., Fujiwara, A, Hirawake, T. and Aoyama, M.: Water mass characteristics and temporal changes in a biological hotspot in the southern Chukchi Sea, Biogeosci., in press., 2016.

Orr, J. C. et al.: Anthropogenic ocean acidification over the twenty-first century and its impact on calcifying organisms, Nature, 437, 681-686, 2005.

Riahi, K., Rao, S., Krey, V., Cho, C., Chirkov, V., Fischer, G., Kindermann, G., Nakicenovic, N., Rafaj, P.: RPC 8.5-A scenario of comparatively high greenhouse gas emissions, Climatic Change, 109, 33-54, 2011.

Ries, J. B., Cohen, A. L. and McCorkle, D. C.: Marine calcifiers exhibit mixed responses to CO_2-induced ocean acidification, Geology, 37, 1057-1152, 2009.

Sabine, C. L., Key, R. M., Johnson, K. M., Millero, F. J., Poisson, A., Sarmiento, J. L., Wallace, D. W. R. and Winn, C. D.: Anthropogenic CO_2 inventory of the Indian Ocean, Global Biogeochem. Cycles, 13, 179-198, 1999.

Springer, A. M., and McRoy, C. P.: The paradox of pelagic food webs in the northern Bering Sea-III. Patterns of primary production, Continental Shelf Res., 13, 575-599, 1993.

Salisbury, J., Green, M., Hunt, C., and Campbell, J.: Coastal acidification by rivers: A new threat to shellfish, Eos Trans AGU, 89, 513, 2008.

Talmage, S. C., Gobler, C. J.: The effects of elevated carbon dioxide concentrations on the metamorphosis, size, and survival of larval hard clams (Mercenaria mercenaria), bay scallops (Argopecten irradians), and Eastern oysters (Crassostrea virginica), Limnol. Oceanogr. 54, 2072-2080, 2009.

Raven, J., et al.: Ocean acidification due to increasing atmospheric carbon dioxide, Report to The Royal Society, 68pp., 2005.

Weingartner, T. J., Cavalieri, D. J., Aagaard, K., and Sasaki, Y.: Circulation, dense water formation, and outflow on the northeast Chukchi shelf, J. Geophys. Res., 103, 7647-7661, 1998.

Woodgate, R. A., Aagaard, K., and Weingartner, T. J.: Monthly temperature, salinity, and transport variability of the Bering Strait through flow, Geophys. Res. Lett., 32, L04601, doi:10.1029/2004GL021880, 2005.

Yamamoto-Kawai, M., Tanaka, N., and Pivovarov, S.: Freshwater and brine behaviors in the Arctic Ocean deduced from historical data of $\delta^{18}O$ and alkalinity (1929–2002 AD), J. Geophys. Res., 110, C10003, doi:10.1029/2004JC002793, 2005.

Yamamoto-Kawai M., McLaughlin, F. A., Carmack, E. C., Nishino S., Shimada K.: Aragonite Undersaturation in the Arctic Ocean: effects of ocean acidification and sea ice melt, Science, 326, 1098-1100, 2009.

Yamamoto-Kawai, M., McLaughlin, F. A., Carmack, E. C.: Effects of ocean acidification, warming and melting of sea ice on aragonite saturation of the Canada Basin surface water, Geophys. Res. Letts., 38, doi:10.1029/2010GL045501, 2011.

Yamamoto-Kawai, M., McLaughlin, F., Carmack, E.: Ocean acidification in the three oceans surrounding northern North America, J. Geophys. Res.,118, doi:10.1002/2013JC009157, 2013.

Yamamoto-Kawai, M., Kawamura, N., Ono, T., Kosugi, N., Kubo, A., Ishii, M., and Kanda, J.: Calcium carbonate saturation and ocean acidification in Tokyo Bay, Japan, J. Oceanogr., 71, 427-439, 2015.

Yao, W., and Byrne, R. H.: Simplified seawater alkalinity analysis: use of linear array spectrometers, Deep Sea Res., 45, 1383-1392, 1998.

Yun, M. S., Whitledge, T. E., Kong, M., and Lee, S. H.: Low primary production in the Chukchi Sea shelf, 2009, Continental Shelf Res., 76, 1-11, 2014.

Figure captions

Figure 1. Distribution of Ωar (a and c) and Ωca (b and d) in bottom water in September/October 2012 (a and b) and July 2013 (c and d). Circled stations were undersaturated with $CaCO_3$ minerals. Stations in red polygon were used in Fig. 2. Red arrows indicate mooring sites.

Figure 2. Vertical sections of (a) salinity, (b) temperature (°C), (c) dissolved oxygen (μmol kg^{-1}), (d) Ωar and (e) Ωca. Left panels are for 2012 and right panels are for 2013. See Fig. 1 for locations.

Figure 3 . Relationships between (a) Ωar and temperature, (b) Ωar and salinity, and (c) Ωar and AOU (μmol kg^{-1}). Blue and red dots are for 2012 and 2013, respectively. Black circles indicate bottom water samples.

Figure 4. Time series of salinity (top), temperature (middle; ℃), and dissolved oxygen and AOU (bottom; μmol kg^{-1}). Red symbols indicate ship-based observations. In the bottom panel, dots and squares are ship-based data of dissolved oxygen and AOU, respectively.

Figure 5. Comparison between Ωar estimated from T, S, and AOU, and Ωar observed during ship-based-cruises (a) in 2012 and 2013, and (b) in 2000, 2002, 2006, 2009 and 2010.

Figure 6. Time series of Ωar (top) and Ωca (bottom) reconstructed from mooring data of T, S and AOU. Red symbols indicate ship-based observations. Black and gray lines are Ω and Ω±RMSE (0.36 for aragonite and 0.57 for calcite).

Figrue 7. Time series of Ωar (top) and Ωca (bottom) for cases when atmospheric CO_2 concentration was 280 ppm (blue; pre-industrial period) or 650 ppm (red; 50 years later). See text for details.

Figure 8. Photo of bivalves corrected by a dredge taw near the mooring location during T/S Oshoro-Maru cruise in 2013.

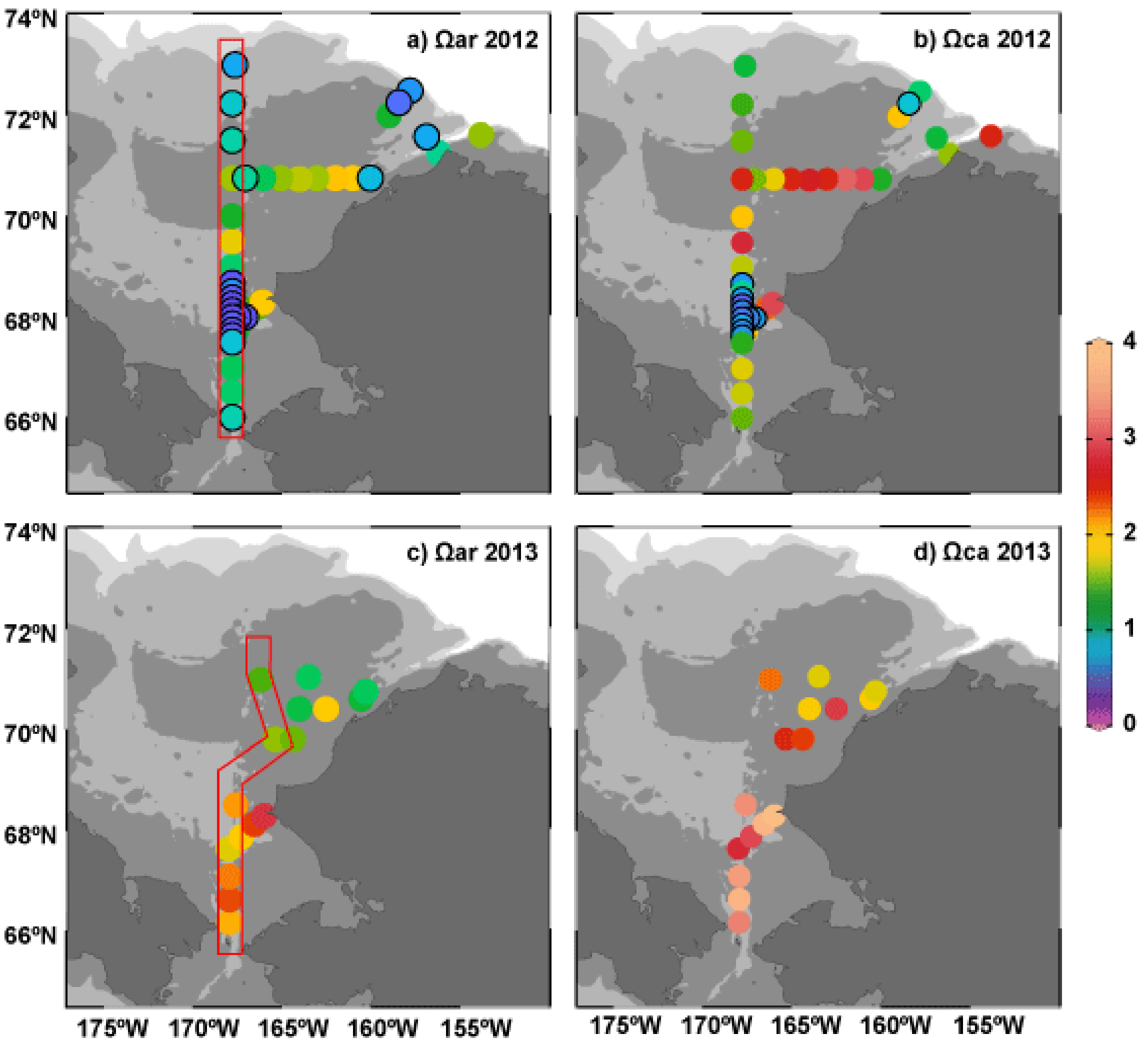

Fig. 1: Distribution of Ωar (a and c) and Ωca (b and d) in bottom water in September/October 2012 (a and b) and July 2013 (c and d). Circled stations were undersaturated with $CaCO_3$ minerals. Stations in red polygon were used in Fig. 2. Red arrows indicate mooring sites.

Biogeosciences Discuss., doi:10.5194/bg-2016-74, 2016
Manuscript under review for journal Biogeosciences
Published: 18 March 2016

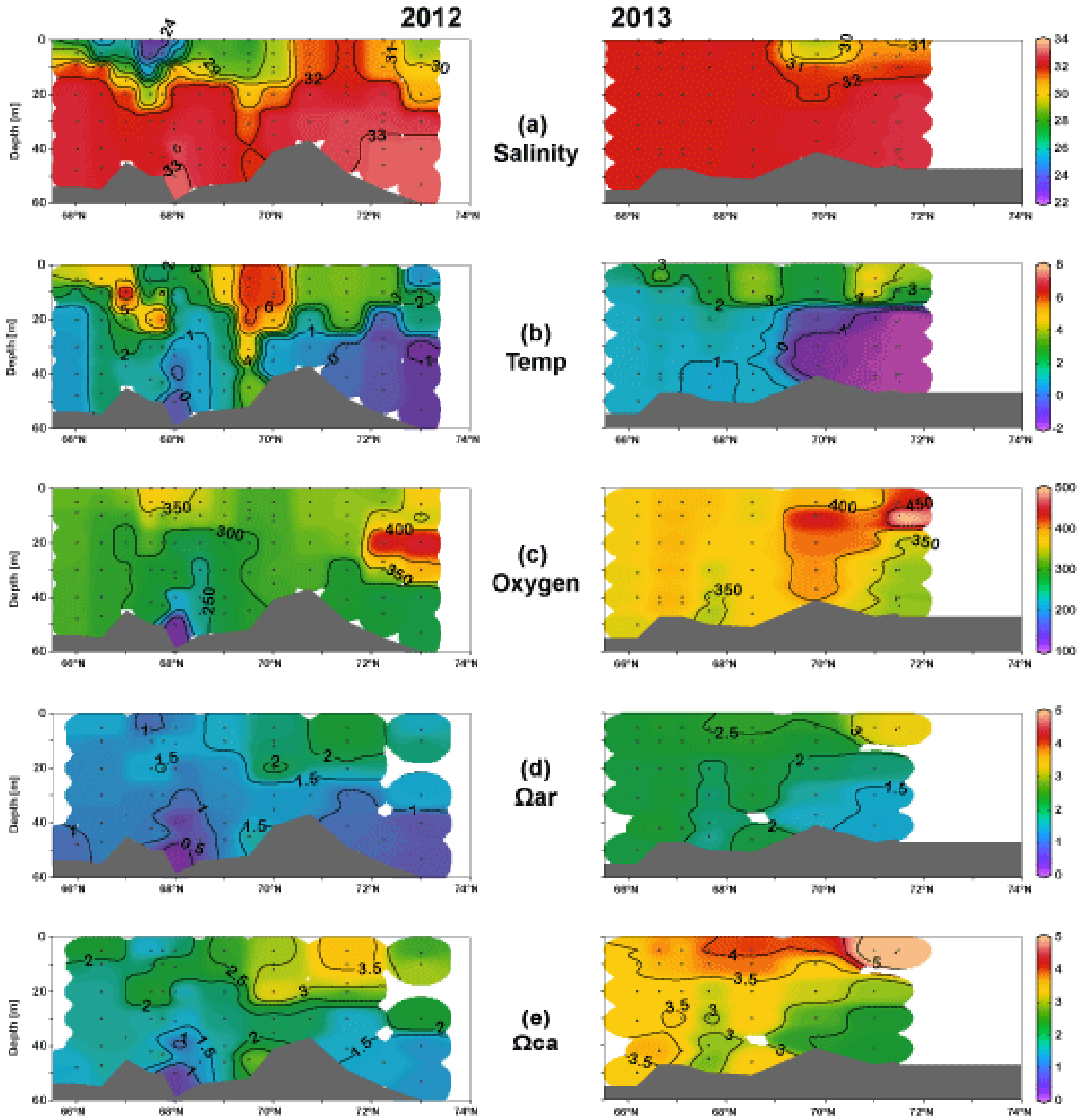

Fig. 2: Vertical sections of (a) salinity, (b) temperature (°C), (c) dissolved oxygen (µmol kg^{-1}), (d) Ωar and (e) Ωca. Left panels are for 2012 and right panels are for 2013. See Fig. 1 for locations.

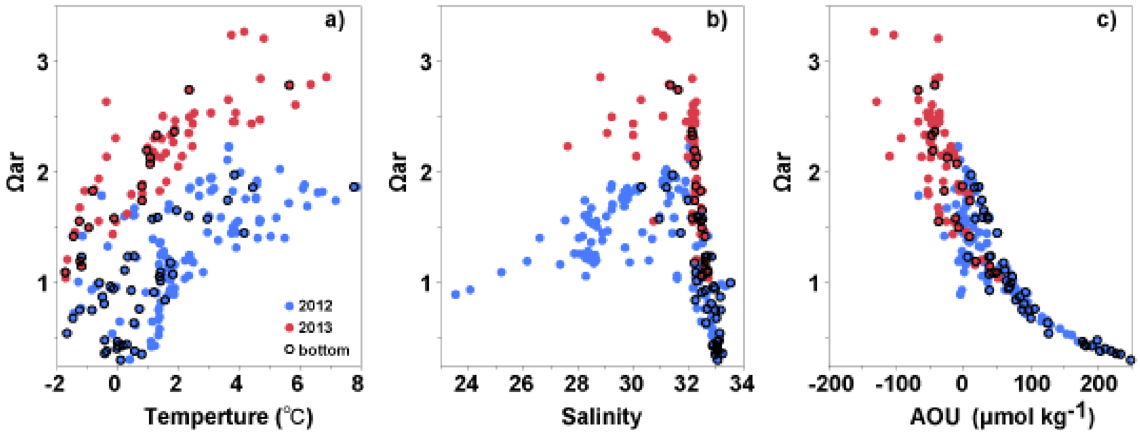

Fig. 3: Relationships between (a) Ωar and temperature, (b) Ωar and salinity, and (c) Ωar and AOU (μmol kg^{-1}). Blue and red dots are for 2012 and 2013, respectively. Black circles indicate bottom water samples.

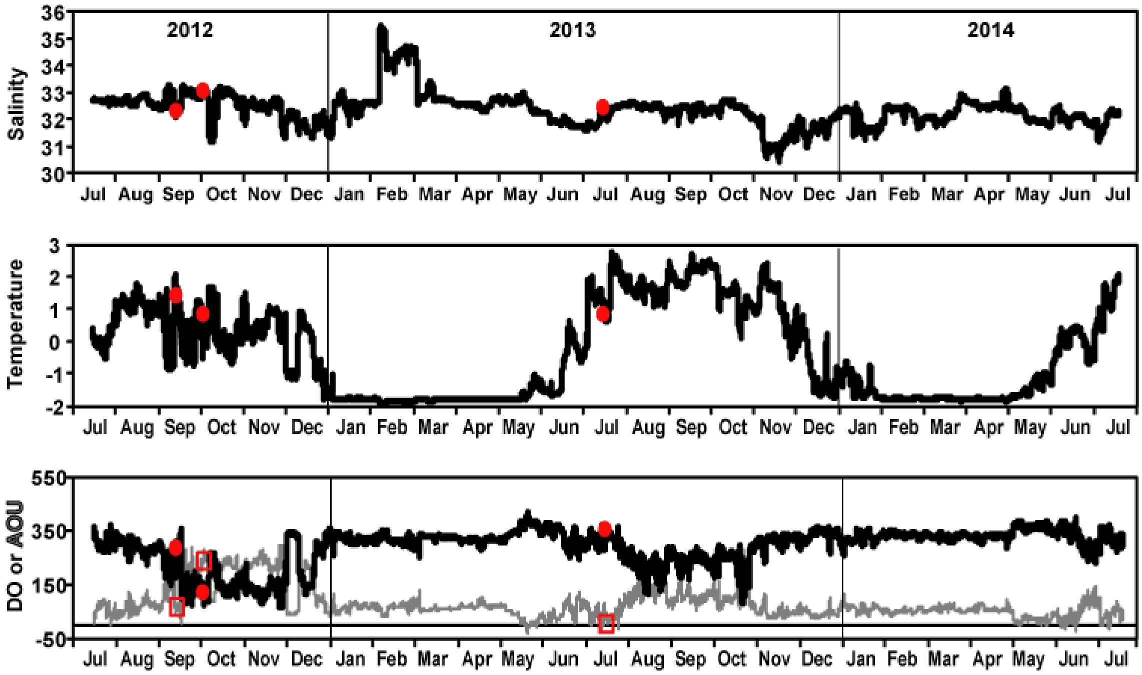

Fig. 4: Time series of salinity (top), temperature (middle; ℃), and dissolved oxygen and AOU (bottom; µmol kg^{-1}). Red symbols indicate ship-based observations. In the bottom panel, dots and squares are ship-based data of dissolved oxygen and AOU, respectively.

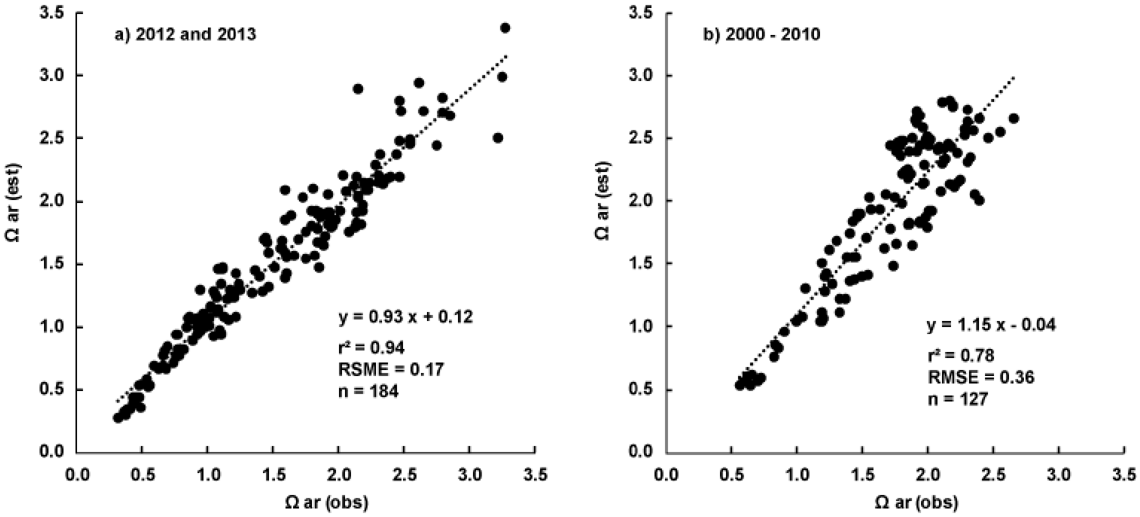

Fig. 5: Comparison between Ωar estimated from T, S, and AOU, and Ωar observed during ship-based-cruises (a) in 2012 and 2013, and (b) in 2000, 2002, 2006, 2009 and 2010.

Biogeosciences Discuss., doi:10.5194/bg-2016-74, 2016
Manuscript under review for journal Biogeosciences
Published: 18 March 2016

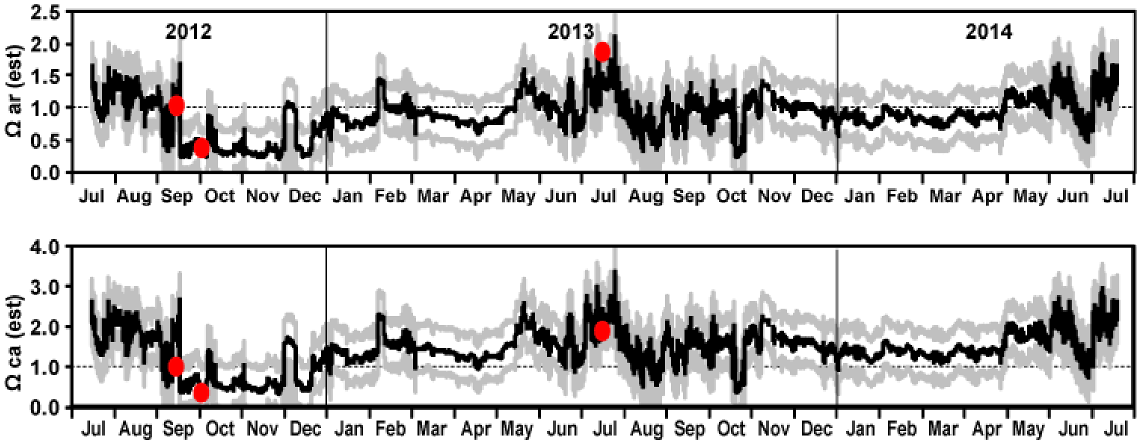

Fig. 6: Time series of Ωar (top) and Ωca (bottom) reconstructed from mooring data of T, S and AOU. Red symbols indicate ship-based observations. Black and gray lines are Ω and Ω±RMSE (0.36 for aragonite and 0.57 for calcite).

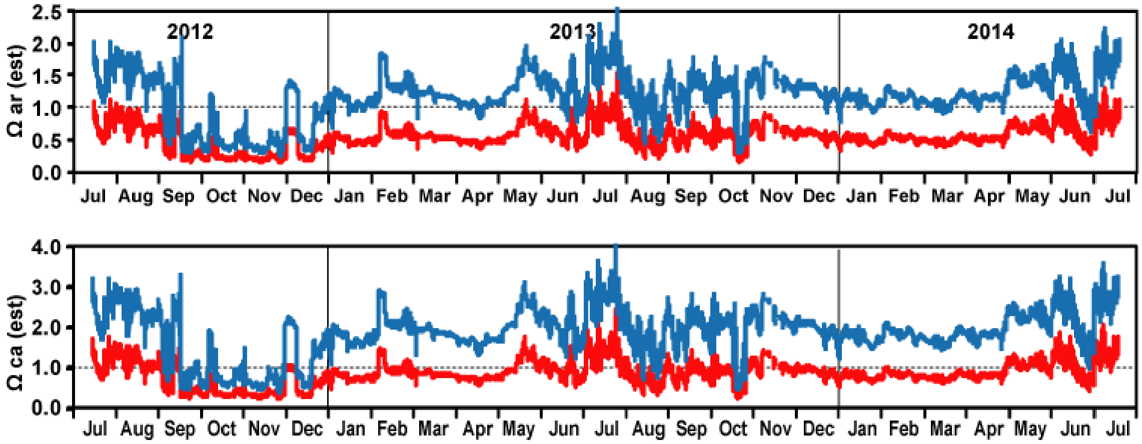

Fig. 7: Time series of Ωar (top) and Ωca (bottom) for cases when atmospheric CO_2 concentration was 280 ppm (blue; pre-industrial period) or 650 ppm (red; 50 years later). See text for details.

Fig. 8: Photo of bivalves corrected by a dredge taw near the mooring location during T/S Oshoro-Maru cruise in 2013.